Bulletin of Earthquake Engineering (2019) 17:4575–4599
https://doi.org/10.1007/s10518-018-0478-6



# A comprehensive in situ and laboratory testing programme supporting seismic risk analysis of URM buildings subjected to induced earthquakes

**F. Graziotti[1,2] · A. Penna[1,2] · G. Magenes[1,2]**

Received: 29 June 2018 / Accepted: 17 September 2018 / Published online: 24 September 2018


**Abstract**
The reliability of a risk assessment procedure is strictly dependent on the adopted hazard, exposure, fragility and consequence models. This paper presents the methodology adopted to support the assessment of the seismic vulnerability of buildings in the Groningen province of the Netherlands by means of a comprehensive in situ and laboratory testing programme. The area, historically not prone to tectonic ground motions, experienced seismic events induced by gas extraction and subsequent reservoir depletion in the last decades. The peculiarity of the input ground motions, the distinctive features and a general lack of knowledge on the seismic response characteristics of the Dutch building stock, and the goal to also assess the collapse risk drove the design and execution of a comprehensive test campaign comprising in situ tests and full-scale shaking table tests of buildings. An overview of the whole campaign is presented, focusing on the merits and roles of the different experimental techniques. The main outcomes of the experimental tests are summarized and additional and wider research findings together with potential research avenues for future studies are also identified.

**Keywords** In situ test · Quasi-static test · Shake-table test · Unreinforced masonry · Structural response · Induced seismicity

## 1 Introduction

The province of Groningen, in the northern Netherlands is not prone to tectonic earthquakes, but has recently experienced seismic events induced by the exploitation of the large gas field that extends under the region (Bourne et al. 2015; Bommer et al. 2016).

✉ F. Graziotti
francesco.graziotti@unipv.it

1 Department of Civil Engineering and Architecture, DICAr, University of Pavia, Via Ferrata 3, 27100 Pavia, Italy

2 European Centre for Training and Research in Earthquake Engineering, EUCENTRE, Via Ferrata 1, 27100 Pavia, Italy

Local structures, mostly unreinforced masonry (URM), were exposed to low intensity motions causing minor damage. Seismicity induced by various human-related activities has been studied for several decades (a comprehensive review may be found in Gillian et al. 2018) while its effects on structures has been poorly investigated. This called for a large research effort aimed specifically at evaluating the vulnerability of the building stock (Crowley and Pinho 2017; Crowley et al. 2018), whose specific focus was on URM buildings; also because of very limited information available on the seismic performance of structures with characteristics comparable with those of the Groningen province. An extensive experimental campaign launched in 2014 aimed at investigating the performance of masonry components, assemblies, structural members and building prototypes with the aim of improving numerical models and analytical predictions.

Several factors characterized this study as innovative and original. They include but are not limited to:

- the very limited knowledge of the seismic behaviour of the building stock, which was never conceived and built for earthquake resistance, and presents characteristic structural solutions (e.g. cavity walls, high slenderness of piers, lack of effective connections, flexible diaphragms, very large openings) which did not even allow a complete and satisfactory reference to available studies on the response of these structures to tectonic earthquakes;
- the lack of information on the effect of low-magnitude and short-duration induced earthquake signals, including magnitudes smaller than 4 usually not considered in engineering design (Bommer and Crowley 2017), on buildings which were designed and constructed without any provision for lateral resistance against seismic shaking (Dost et al. 2018);
- the need for estimating the "Local Personal Risk" of buildings, defined as the annual probability of fatality for a hypothetical person continuously present inside or within 5 metres of a building (Crowley et al. 2017b; van Elk et al. 2017). This required a robust estimate of the collapse probability of structural and non-structural elements within a building, which implied consideration of uncertainties higher than those associated with other damage states. The challenging design of experimental tests allowed for the execution and interpretation of collapse shake-table tests on structural components and building prototypes.

The experimental programme performed by EUCENTRE, LNEC and Delft University of Technology (TU Delft) included in situ mechanical characterisation tests (Tondelli et al. 2015) and laboratory tests, such as: (1) characterisation tests on bricks, mortar and small masonry assemblies; (2) in-plane cyclic shear-compression tests (Graziotti et al. 2016a) and dynamic out-of-plane tests on full-scale masonry piers in one- and two-way bending (Graziotti et al. 2016b, 2018a); and (3) full-scale unidirectional and bidirectional shake table tests on different URM building typologies (Graziotti et al. 2017; Kallioras et al. 2018b; Tomassetti et al. 2018a; Correia et al. 2018; Kallioras et al. 2018a). An overview of the experimental campaign on URM structures is reported in the following sections, focusing on motivations, methodology, results, observations and possible use of all the acquired knowledge. A summary of the tests performed at TU Delft is reported in Messali et al. (2018).

It is noted that, within the framework of the seismic risk assessment for Groningen, a parallel experimental campaign, similar in scope but smaller in extent, was deployed also for those type of Groningen reinforced concrete structural systems for which experimental or numerical seismic response data was not available. Details on such activities, which were beyond the scope of this manuscript, can be found in Brunesi et al. (2018a, b, c).

### 1.1 Description of the testing programme

The testing campaign was specifically designed to support the development of the risk engine used in the framework of a project aimed at assessing the induced seismicity risk for the Groningen gas field (NAM 2016). Crowley et al. (2017b) clearly stated the needs of a risk analysis for the assessment of the "Local Personal Risk", including fragility models robustly estimating the probability of collapse of structural and non-structural elements within a building, for the estimation of casualties for a scenario earthquake, and consequence models requiring estimates of the amount of collapsed debris to provide the probability of injury or death to people hit by this debris. The experimental campaign was specifically designed to provide the information needed to define numerical models capable of predicting the response of structures up to collapse conditions, to be used in the calibration of the vulnerability models embedded in the engine used to compute the seismic risk.

Figure 1 represents a scheme of the risk engine adopted by Crowley et al. (2017b); the dashed box includes the processes that benefited from the experimental campaign while the grey solid one includes information used to plan the tests.

In order to design the tests, particularly for the shake table ones, seismological information is essential to apply time histories representative of those that may hit the building stock to be assessed. Particular attention was paid to the selection of the most appropriate input motions, not only in terms of spectral shape but also taking into account other intensity measures specific of earthquakes induced by this gas field (i.e. peak ground velocity and significant duration). Furthermore, data on building typology, mechanical properties and detailing were necessary to set up the most appropriate tests on component and structures, in order to take advantage of the tested seismic response of structures similar to those of the building stock and subjected to motions compatible with those that could potentially hit the region.

On the other hand, the test campaign served as input for the calibration of an exposure model, fragility functions and consequence model. All the data collected and elaborated from the laboratory tests constituted a reliable reference for the calibration of numerical models simulating the static and dynamic behaviour of structures or part of them (e.g. Kallioras 2017; Avanes et al. 2018; Malomo et al. 2018b, c; Tomassetti et al. 2018b). Particular attention was focused on the testing and subsequent collapse simulations of structures to develop the consequence model; shaking-table collapse tests were performed at LNEC laboratory on full-scale buildings and at EUCENTRE on specific structural components.

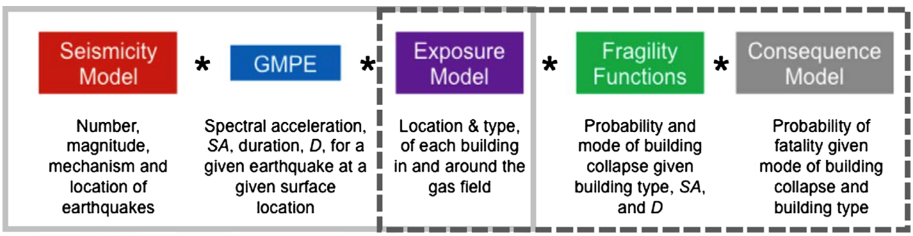


**Fig. 1** Components of the calculation of local personal risk (adapted from Crowley et al. 2017a, b)

Numerical models generated taking the lessons learned during the testing and calibration process into account were used to run nonlinear dynamic analyses and estimate fragility functions of different building typologies (Crowley et al. 2017a). Engineering demand parameters representing various limit states (e.g. damage and collapse) were identified analysing the test results.

Masonry properties can be very susceptible to variability due to workmanship. This factor should be isolated and treated independently along with other test variables and typically laboratory tests should seek to reflect uniform conditions of workmanship. Although real buildings are not built with such strict control, it is desirable to limit the possible causes of scatter especially when tests are used to validate numerical models (Calvi et al. 1996). In order to limit this variability but in the same time guaranteeing the representativeness of the specimens, Dutch masons were employed to construct the specimens. The material and geometrical properties of the reference building numerical models were extended to be compatible with the exposure model, which was developed taking into account the results of the in situ material testing performed on the building stock. Table 1 reports a brief summary of the experimental campaign started in 2014 and completed to-date. The section of the paper describes each of the tests performed is also specified together with the components of risk engine that benefited from each test typology. In order to allow interested researchers study or model the tests conducted, all data recorded by EUCENTRE and LNEC and the videos of the majority of the tests can be requested online at www.eucentre.it/nam-project.

## 2 Tests on masonries of the building stock

The main objective of in situ material testing within this project was to provide a set of masonry properties to be used as input for numerical models, used as a reference for the development of fragility curves and also as input for the design of full-scale tests on replicated buildings (e.g. see Sect. 4.2). Arbitrary assumptions on material properties generally increase the uncertainties of the predictions if not supported by reliable experimental data.

Since the information on the mechanical characteristics of the masonry in the Groningen area was very limited, 16 buildings, comprising residential structures and schools, dating from the early 1920s to 2005, were selected and tested. The tested walls included both clay and calcium silicate brick masonry of various qualities and conditions. In situ testing, performed by P&P Consulting Engineers under the supervision of EUCENTRE, included non-destructive tests such as rebound hammer and sonic tests, and semi-destructive test, i.e. flat jack and shove test. Furthermore, samples were carefully extracted to be taken to the laboratory, where the destructive campaign comprising compressive, flexural, shear and bond wrench tests was performed by TU Delft and Eindhoven University of Technology (TU/e) laboratories.

Despite of the limited number of sampled buildings, the part of the campaign provided a better insight into the researched material and the formulation of a preliminary masonry catalogue for the region. The available data suggest that the use of sub-typologies (e.g. depending of the masonry quality or condition) could reduce the dispersion on the results (Zapico Blanco et al. 2018). Detailed information about the mechanical characteristics of the tested masonry is provided by Tondelli et al. (2015). Laboratory tests included compression and bending tests on bricks and mortar, compression tests on masonry, shear tests on masonry and bond wrench tests (Jafari et al. 2017); the tests were performed according

**Table 1** Summary of the experimental campaign and impact on the risk model

| Type | Tested specimens | Nr. of tests | Performed by | Main outcome | Further development | Section | Exp. | Frag. | Conseq. |
|---|---|---|---|---|---|---|---|---|---|
| On building stock | In situ and extracted wallettes and triplets  | 16+ buildings, 500+ tests | EUCENTRE, TU Delft, TU/e, P&P C. Eng. | Mechanical properties catalogue of the building stock | Expand the database | 2 | X | X | |
| Quasi-static | Wallettes, triplets, mortar, bricks  | 500+ | EUCENTRE, TU Delft | Detailed mechanical characterisation of each full-scale test, input for numerical modelling | Study possible correlation between mech. parameters | 3.1 | | X | |
| | Piers in-plane 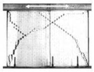 | 15+ | EUCENTRE, TU Delft | Behaviour of piers loaded in plane, identification of limit states | Tests with different materials and boundary conditions | 3.2 | | X | |
| | Walls out-of-plane  | 20+ | TU Delft, EUCENTRE | Behaviour of walls loaded out-of-plane | Validate analytical/numerical formulations, define a post-peak behaviour, study correlations of mech. parameters | 3.2 | X[a] | X | |
| | Full-scale structure  | 3 | TU Delft, LNEC | Cyclic behaviour of structures and assemblages | | 3.3 | | X | |
| Dynamic shake table | Walls out-of-plane  | 14 | EUCENTRE | Out-of-plane dynamic and collapse behaviour of walls | Validate analytical/numerical formulations, define a post-peak behaviour | 4.1 | | X | X |
| | Full-scale assemblage  | 1 | LNEC | Dynamic and collapse behaviour of timber roof | Test different configurations | 4.2 | | X | X |
| | Full-scale structure  | 5 | EUCENTRE, LNEC | Dynamic and collapse behaviour of structures, define limit states and debris area | Test different configurations | 4.2 | | X | X |

[a]Further development

to the same standards used in replicated masonry tests (see Sect. 3.1). As a consequence of the limited number of tested samples, no statistical distribution for the mechanical parameters could be derived and only the average value, the coefficient of variation and the minimum and maximum value measured during the campaign were proposed as results.

Each building was also subjected to in situ testing. While the laboratory tests are in general more accurate and complete, the in situ campaign is typically cheaper, faster and much less disruptive. Furthermore, testing in situ adds the unknowns of a not completely controlled environment, but eliminates the non-negligible effects of the samples cutting and transportation, and allows the testing of very poor quality masonry which would be impossible to be brought to the laboratory.

The entire in situ campaign is organized into semi-destructive tests i.e. single/double flat jack and shove tests (according to ASTM guidelines, ASTM 2014a, b, 2016), and non-destructive tests i.e. rebound hammer test, penetrometric test on mortar and sonic test. A complete list of the performed tests can be seen in Table 2, together with the main properties obtained and their possible correlations with other properties.

### 2.1 Additional and wider research findings

The tests performed in this phase of the project gave the opportunity to study aspects beyond the creation of the masonry catalogue. In particular, the analysis of the data (mean and C.o.V.) allowed studies on the intra-building and the inter-building mechanical properties variability. Furthermore, the direct comparison of in situ and lab tests pointed out some inconsistencies, in particular in the ASTM C1531 (ASTM 2016) interpretation of the shove test. Complementary works by Rossi et al. (2015), Bonura et al. (2018), Andreotti et al. (2018) allowed the proposal of a new procedure proposed to ASTM committee (Graziotti et al. 2018b).

## 3 Quasi-static tests

Quasi-static tests on structural components and assemblages represent an essential source of information in assessing the behaviour of masonry structures subjected to horizontal loading. Although it is well known that while the seismic excitation can be simulated by means of dynamic tests, quasi-static tests allow an accurate investigation of several interesting aspects: a precise observation and monitoring of the damage propagation, direct and accurate measurement of the forces, direct evaluation of hysteretic energy dissipation, identification of damage levels and also calibration of reliable numerical models in term of force–displacement response. It is important to keep in mind the fact that masonry exhibits a rate-dependent behaviour: because propagation of cracking at constant load or at constant imposed displacement is often observed, quasi-static tests tend to induce more extensive damage than dynamic tests, which ultimately results in lower measured strength (Calvi et al. 1996).

### 3.1 Complementary characterisation tests

Complementary tests performed in the framework of full-scale tests on components or buildings are essential in order to fully characterize the masonry composing the primary specimen. One major scope of full-scale tests (at least in a project like this) is to calibrate numerical models to perform further analyses. Reducing the uncertainties in terms of boundary conditions, input, mechanical and geometrical characteristics is essential in order to obtain a reliable calibration of numerical models.

For this reason, extensive mechanical characterisation campaigns were conducted in parallel with all the full-scale tests performed.

Both units and mortar were characterized in terms of their compressive ($f_b$ and $f_c$) and flexural strengths ($f_{bt}$ and $f_t$) following procedures compliant with the relevant norms i.e. EN 772-1 (2011) (Fig. 2a, b) for units and EN 1015-11 (1999) for mortar. Masonry as an assemblage was characterized in terms of its elastic modulus $E_m$, compressive strength $f_m$, in-plane and OOP flexural strengths $f_{x3}$, $f_{x2}$ (Fig. 2e–g); flexural tensile strength of masonry or bond strength $f_w$ (Fig. 2h) and cohesion $f_{v0}$ and friction coefficient $\mu$ in shear. All of the aforementioned characterisation tests were performed in compliance with existing European norms i.e. EN 1052-1 (1998), EN 1052-2 (1999), EN 1052-5 (2005), EN 1052-3 (2002). Additionally, for the OOP two-way bending experimental campaign, the tested masonry was also characterized under torsional shear using a novel technique and setup designed and performed by Graziotti et al. (2018a).

Table 3 summarises the results of the complementary characterisation tests performed for a building representative of a pre-1940 Groningen clay-brick masonry tested dynamically by Kallioras et al. (2018b). This table compares the results of the performed laboratory characterisation tests with values obtained from in situ testing on pre-1940 clay-brick masonry buildings, which include both intra-building and the inter-building variability. The values obtained from laboratory characterisation tests are comparable to the parameters obtained in situ i.e. material properties of the house can be considered representative of the building stock being studied. An exception arises here only in the case of compressive strength of units ($f_b$) and Young's modulus ($E_m$) which exceed average values obtained from the experimental campaign but are still lower than maximum values obtained in situ (Tondelli et al. 2015).

### 3.1.1 Additional and wider research findings

The extensive experimental campaign gave the unique opportunity to test and characterize different types of masonry in terms of materials and bond patterns. Additionally, the repetition of tests on nominally identical specimens, allowed the highlighting of how some of the mechanical properties are strongly influenced by the maturation conditions. For example, temperature and humidity strongly influenced the tensile strength $f_w$ of nominally-identical calcium silicate masonry that resulted to be as low as 0.05 MPa for specimens built in summer and went up to 0.95 MPa for specimens built in winter.

Furthermore, the repetitive companion characterisation tests allowed to correlate different parameters of the same masonry built at the same time with identical materials. For example, although the large amount of research on the behaviour of URM under the action of uniform shear stress at the brick mortar interface, very limited research exists on the response of bed joints in masonry under torsional shear where the distribution of shear stress is non-uniform. This is despite the fact that torsional shear resistance is one of the most important controlling parameters in virtual work based methods (Vaculik 2012) that constitute the existing state of the art analytical formulation applied to URM loaded in the OOP direction. Consequently, a novel characterisation test was planned in order to evaluate the response of masonry bed joints under combined torsion and

**Table 2** In situ testing campaign and related properties (Zapico Blanco et al. 2018)

| | Measured property | Derived properties |
|---|---|---|
| Single flat jack test | Compressive stress in the masonry | |
| Double flat jack test | Masonry vertical Young's modulus | Compressive strength of masonry can be derived |
| Shove test | Mortar joints shear strength for bed joint (cohesion) and friction angle | |
| Rebound hammer test | Info on masonry homogeneity | Compressive strength of bricks can be derived through correlation with other tests |
| Penetrometric test on mortar | Qualitative strength mortar | Compressive strength mortar can be derived |
| Ultrasonic test | Info on masonry homogeneity | Stiffness of masonry can be derived |

compression. As for the shear strength, the results of these tests were also represented in a Coulomb-type friction law representation after performing linear regression in order to obtain corresponding values of initial shear strength ($f_{v0,tor}$) and coefficient of friction ($\mu_{tor}$) under torsional shear. An experimental study is now taking place to try to correlate these parameters with the masonry tensile strength $f_w$, the bed-joint cohesion $f_{v0}$, and the shear friction coefficient, $\mu$.

### 3.2 Quasi-static tests on components

Quasi-static tests on structural components represent an essential source of information in assessing the behaviour of masonry structures subjected to in-plane and out-of-plane horizontal loading. This part of the campaign focused on assessing both the in-plane and out-of-plane behaviour of Dutch masonry typologies by applying quasi-static cyclic loading in displacement control. Tested specimens involved a total of 15 in-plane and more than 20 out-of-plane tests carried out on calcium silicate and clay masonry piers (with different aspect ratios, bond patterns, boundary and loading conditions). Part of these tests have been performed at the TU Delft lab, in particular the quasi-static airbag out-of-plane tests and some of the in-plane tests (Messali et al. 2017) Out-of-plane horizontal bending tests on smaller components have also been performed by EUCENTRE; these quasi-static tests were performed deforming out-of-plane several $1.8 \times 0.7$ m specimens by means of a servo-hydraulic actuator to study the effect of torsional strength on horizontal bending of solid-brick URM (see Sect. 3.1.1).

For what concerns the cyclic in-plane tests performed at EUCENTRE, different local damage levels were identified taking the structural damage observed through the different testing stages and the force/displacement curves into account: Fig. 3 reports the testing setup and, as an example, the identification of the local damage limits on the envelope curve of one of the tested calcium silicate slender wall ($2.75 \times 1.1 \times 0.1$ m, double-fixed with vertical stress of 0.7 MPa); in particular, $\theta_{cr}$ is the drift associated with the formation of the first visible cracking, $\theta_{Vmax}$ the one corresponding to the peak strength, $\theta_u$ the one associated with a drop in shear force of 20% and $\theta_{NC}$ the drift corresponding to the loss of bearing capacity. In this case, the last three drifts assume the same value due to the development of a rocking mechanism without softening.

### 3.2.1 Additional and wider research findings

A relevant result from this test is the relatively high energy dissipation capacity developed by the calcium silicate walls, despite the activation of a prevailing rocking mechanism, as the one shown in Fig. 3. Studies were also conducted on the influence of the loading protocol (i.e. number of repetitions per cycle) on the definition of limit states (Mandirola et al. 2017), an aspect that could be particularly relevant considering the short significant duration of the induced seismicity earthquakes.

## 3.3 Quasi-static tests on full-scale structural assemblies

Isolated structural component tests are the most direct and cost-effective means to understand structural behaviour; however, it was necessary on occasions to test a complete structural system to observe the response of the components under realistic combinations of actions (applied displacements, rotations, shear, bending moment, and axial load), and verify analytical models applied to complex systems (Calvi et al. 1996).

It is of primary importance to select subsystems which could represent realistic structural configurations and yet be simple enough to be effectively modelled to study the behaviour under investigations. In order to reduce the uncertainties in the modelling phase,

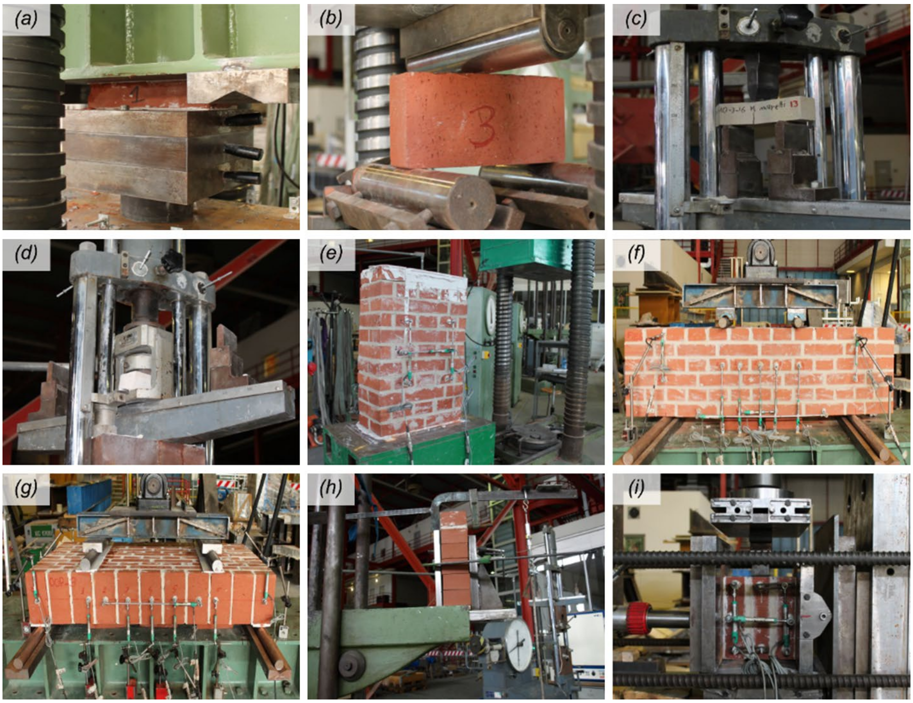


**Fig. 2** Mechanical characterisation tests: **a** compression test on a clay brick; **b** three-points bending test on a clay brick; **c** three-points bending test on a mortar specimen; **d** compression test on a mortar specimen; **e** compression test on a masonry wallette; **f** four-points in-plane bending test; **g** four-points out-of-plane bending test; **h** bond wrench test; **i** shear test on a triplet (Kallioras et al. 2018b)

**Table 3** Masonry mechanical properties for the building prototype compared to in situ tests on pre-1940s clay-brick URM buildings in the Groningen province (Kallioras et al. 2018b)

| Material property (units) | Building prototype | | In situ tests | |
|---|---|---|---|---|
| | Average | C.o.V. | Average | C.o.V. |
| Density of bricks, $\rho_b$ (kg/m$^3$) | 2101 | 0.02 | – | – |
| Density of masonry, $\rho$ (kg/m$^3$) | 1984 | 0.01 | – | – |
| Brick compressive strength, $f_b$ (MPa) | 46.8 | 0.11 | 25.6 | 0.23 |
| Brick flexural strength, $f_{bt}$ (MPa) | 8.50 | 0.05 | 6.43 | 0.64 |
| Mortar compressive strength, $f_c$ (MPa) | 4.12 | 0.24 | – | – |
| Mortar flexural strength, $f_t$ (MPa) | 1.20 | 0.33 | – | – |
| Masonry compressive strength, $f_m$ (MPa) | 9.23 | 0.07 | 8.91 | 0.52 |
| Masonry Young's modulus in compression, $E_{m1}$ (MPa) | 8123 | 0.25 | 5346 | 0.60 |
| Masonry flexural in-plane strength, $f_{x3}$ (MPa) | 0.44 | 0.19 | 0.61 | 0.45 |
| Masonry flexural out-of-plane strength, $f_{x2}$ (MPa) | 0.64 | 0.15 | 0.83 | 0.47 |
| Masonry flexural bond strength, $f_w$ (MPa) | 0.23 | 0.60 | 0.33 | 0.69 |
| Masonry (bed-joint) cohesion, $f_{v0}$ (MPa) | 0.15 | – | 0.28 | 0.26 |
| Masonry (bed-joint) shear friction coefficient, $\mu$ | 0.55 | – | 0.66 | 0.18 |

the boundary conditions, the applied forces, the loading rates, the used materials and the geometries should be well defined and should have a unique interpretation. There are three testing procedures that could be applied to test structures or assemblages: the quasi-static tests (briefly described in this section), the pseudo-dynamic tests, and the shaking table or dynamic tests (described in Sect. 4). In the framework of this project, the first and the last were used.

Given the peculiarity of the different procedures, quasi-static tests should be considered as complementary to shake table dynamic tests. In fact, in quasi-static tests concentrated loads have to be applied idealizing the specimen as an equivalent lumped mass system. For this reason, the out-of-plane behaviour of walls was not taken into account in push-over tests of entire buildings, this needs to be studied performing specific static (e.g. Griffith et al. 2007; Messali et al. 2017 and Sect. 3.2) or dynamic (e.g. Giaretton et al. 2016; Degli Abbati and Lagomarsino 2017; Vaculik and Griffith 2018) component tests. Another drawback of the quasi-static tests is that the displacement or force load pattern has to be decided a priori, forcing the structure to a particular behaviour and not allowing the identification of all the dynamic properties of the specimens (e.g. the damping properties and natural mode shapes). On the other hand, quasi-static tests have full control of the applied forces and displacements allowing the continuous monitoring and correlation of progress of damage with deformations. This is more difficult in dynamic shaking table tests, were the crack propagation is a function of the characteristics and the sequence of input motions. Furthermore, incremental dynamic tests allow the detection of cracking only between runs; this permits to correlate a particular damage state only with a range of deformations and not with a specific threshold (see Table 6). For all these reasons, both static and dynamic testing are essential for a complete study of the behaviour of complex structural systems.

Attention is drawn to two full-scale URM houses subjected to cyclic pushover tests at TU Delft in the framework of the project. Considering that the intention of this test was to validate numerical and analytical methods of structural analysis, only the load-bearing parts of typical terraced house in Groningen were tested while spandrels and veneer were not constructed (Fig. 4). Consequently, the tested structures comprised of four slender piers on the façade which were connected to two long transversal walls. Displacement control was adopted with the additional consideration of maintaining a 1:1 ratio between the forces at the two levels. More information about this experiment can be found in Esposito et al. (2017, 2018).

Another example of a full-scale quasi-static test performed in the framework of the same project is the one performed in the LNEC laboratory (Correia et al. 2018). This test was uncommon not only because it was the first test performed on a complete full-scale roof structure, but also because it was a quasi-static test performed using a shaking table. Following the shaking table test on the complete roof substructure, the remaining URM cavity walls composing the gables were carefully removed and a support timber structure was put in place to allow for additional testing on the timber roof system. A cyclic pushover test could thus be performed using the shake table as actuator system and taking advantage of the particular characteristics of the LNEC shaking table, which is surrounded by three reaction walls. The East and West extremities of the ridge beam were fixed to the reaction walls through steel ties, as shown in Fig. 5. Both steel ties were instrumented with load cells, whereas each of the five timber roof beams was instrumented with a wire potentiometer to measure its horizontal displacement with respect to the reference steel frame. The control system of the shaking table was prepared for using the relative displacement between the reference frame and the ridge beam as control variable, thus ensuring that the desired drift on the specimen was applied at each cycle. The roof structure was then subjected to two full cycles at ± 10 mm, ± 50 mm, ± 100 mm and ± 150 mm. The force-diaphragm drift curve obtained together with other information can be found in Correia et al. (2018). Further quasi static tests on sub-assemblages are envisaged to be performed at EUCENTRE to study the flange effect on U-shaped specimens. In particular, attention will be focused on the vertical load redistribution that could overload the in-plane-excited piers and unload the transverse one excited out-of-plane, increasing the vulnerability of both structural elements and possibly leading to structural collapses, as observed by Tomassetti et al. (2018a).

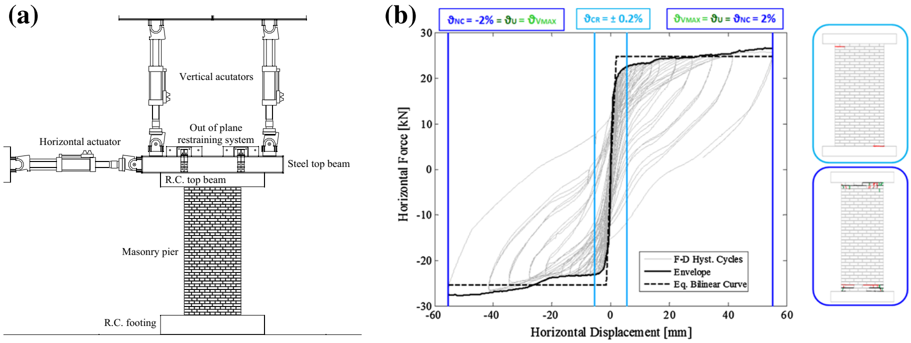


**Fig. 3** Scheme of the test setup for the in-plane cyclic quasi-static tests (**a**); identification of the damage states on the base shear vs horizontal displacement curve for one of the slender calcium silicate pier (**b**) (Mandirola et al. 2017)

## 4 Dynamic tests

Dynamic shaking table tests on full-scale models represent the most complete experiments to study the seismic behaviour of structures and components, especially in the nonlinear range. In these tests, the input is given at the base of the specimen assigning an acceleration/displacement time history to the shake table that is sustaining the construction to be tested. The input motion could be in one direction or in multiple directions (including the vertical one). The distribution of forces in the structure is not given by concentrated load as in the quasi-static tests and their distribution is not defined a priori, but the inertia forces act as distributed load on the structure, allowing, for example, the correct simulation of out-of-plane response of walls and the force distribution is realistically given by the dynamic response of the structure itself. There are also some drawbacks of these tests, not only related to the costs and complexity. For example, a continuative visual monitoring of the damage development is not possible at the moment, the damage states are defined only between tests. Furthermore, as in the vast majority of large-scale tests, these tests accumulate damage in the specimen. This fact has to be seriously taken into account once the test is used as a reference for the calibration of numerical models that most probably are intended to simulate the dynamic response of a non-damaged structure.

The dynamic behaviour and performance of structures as well as the definition of limit states threshold (i.e. engineering demand parameters limits) are influenced by the input motion. For this reason, the selection of the acceleration and displacement time-histories and the definition of their sequence is one of the most critical aspects of these tests. The first aspect to consider is the capability of the shake table to apply the selected record with only minor distortion, in particular in the frequency range of interest (i.e. around the fundamental periods of the structure). Secondly, it is generally better to select a signal easy to reproduce via numerical modelling characterized by a relatively smooth acceleration response spectrum to facilitate the interpretation of its effect on the structure. In particular, in this case of the study of vulnerability of structures subjected to induced seismicity, it is also very important to assign a series of motions with characteristics reflecting the seismicity of the area. This is due to the fact that the dynamic behaviour of a structure going in nonlinear range is not only influenced by the elastic spectrum of the motion but also by factors such as the significant duration (Hancock and Bommer 2006), the peak velocity and the Housner intensity (Housner 1952).

If the shake table test is executed well and all the data reliably recorded, the amount of information that is possible to obtain from this type of experiment is very large. Among these, of primary importance is damage pattern evolution, fundamental period degradation and the collapse mechanism. Furthermore, a full-scale dynamic test is a unique opportunity to associate damage states with engineering demand parameters such as the interstorey drift or even ground motion parameters. Another important output of these tests are hysteretic plots of the entire structure or a part of it such as the roof subsystem. These plots together with deformed shapes give the opportunity to study the dynamic behaviour of the specimen in terms of dissipated energy, displacement demand, displacement capacity, strength capacity and in general provide reference for detailed numerical modelling and calibrations. All recorded data (acceleration and displacement time histories) and videos of the majority of shaking table tests were made available upon request to all researchers interested in studying and/or modelling the dynamic behaviour of the tested specimens (online requests at www.eucentre.it/nam-project).

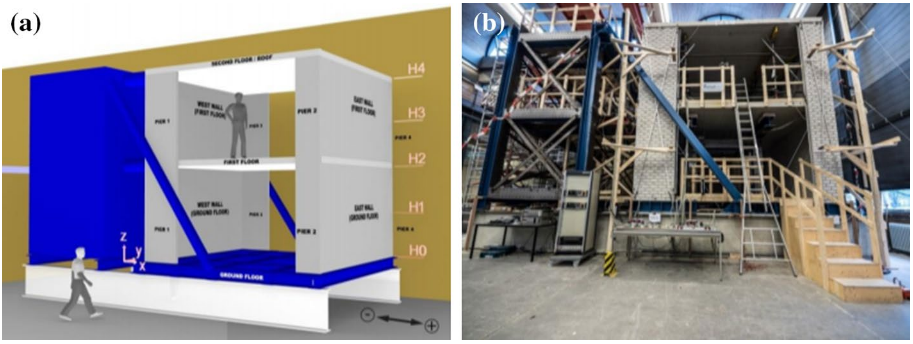


**Fig. 4** Set-up and specimen of quasi-static test conducted at TU Delft lab: **a** 3D representation and **b** picture (Esposito et al. 2017)

## 4.1 Out-of-plane dynamic tests on components

Activation of local out-of-plane mechanisms has been identified as a major cause of structural collapse from experience in past and recent seismic events. Cavity walls which represent a commonly used structural system throughout the Groningen province as well as Central and Northern Europe, China, New Zealand and Australia are found to be particularly vulnerable. In such structural systems, the inner leaf has a load-bearing function while the outer veneer serving aesthetic and insulation functions is usually lightly loaded. Despite their high reported vulnerability, very less experimental data (especially dynamic tests) can be found on cavity walls in literature (e.g. Giaretton et al. 2016), in fact none can be found for a two-way-bending configuration. Consequently, 14 full-scale unreinforced masonry walls were tested dynamically by Graziotti et al. (2016b, 2018a).

An experimental setup was specifically designed for this purpose, allowing the full-scale specimens to be tested with different input signals imposing out-of-plane one-way and two-way bending right up to collapse of the specimens. Special considerations were adopted to ensure that the boundary conditions of the experiment were always known and could be easily idealized, for example, pre-compression was always applied with a spring system that ensured increase in the applied pre-compression never exceeded more than 5% of the initial


**Fig. 5** Pictures of the roof specimen tested at LNEC: support and guidance system and steel ties connecting the ridge beam to the reaction walls (Correia et al. 2018)

static force. Such considerations were employed despite the knowledge that they were not necessarily representative of the actual actions occurring in a building subjected to ground motions as the intention of these experiments were to calibrate numerical models.

The input motions were also selected to be representative of the floor motions of a typical terrace house of the Groningen province subjected to induced seismicity. When available (i.e. for the two-way-bending tests), the applied motions were those recorded at the floor level during the tests of the full-scale building on the shake table (see Sect. 4.2). For the one-way bending tests, performed before the tests on building, the filtering effect of the structure was simulated by means of a numerical model (Lagomarsino et al. 2013). All these floor motions took into account the damage progression in the primary structure; generally, the floor spectra associated with a damaged building is less amplified in terms of maximum acceleration but it is characterized by a "wider" spectra (i.e. longer corner period). Other inputs were also applied in order to facilitate the calibration of analytical and numerical models (e.g. Tomassetti et al. 2018b; Malomo et al. 2018a) as, for example, a Ricker Wave Acceleration input, which consists of a particular acceleration pulse.

Table 4 and Fig. 6 summarize the configurations of the specimens tested on the EUCENTRE shaking table in between 2015 and 2018. In Fig. 7 pictures of collapses of the one-way-bending specimens are reported. For all specimens which were not laterally restrained i.e. without return walls, failure occurred with the formation of classical top, bottom and mid-height hinges and the walls exhibiting one-way bending/rocking behaviour. Despite the negligible flexural stiffness of the ties used between the leaves of the cavity wall and the poor mechanical characteristics of the mortar used for CS walls, they ensured compatibility in the horizontal displacement response of both the leaves even when they were used at density of 2 ties/m$^2$. It is interesting to notice that all tested cavity walls specimens with unloaded external clay-masonry veneer exhibited lower capacities than their constituent leaves subjected to the same pre-compression (on the calcium-silicate masonry wall). More information on these experiments can be found in Graziotti et al. (2016b).

Regarding the two-way bending tests, crack patterns were highly influenced by the differences between mechanical properties of masonry types. Specimens showed a relatively brittle behaviour after the attainment of first cracking, with a failure acceleration lower than the cracking one. Further information can be found in Graziotti et al. (2018a). A second set of three specimens was recently tested trying to investigate the influence of vertical floor motion on the behaviour of walls excited out-of-plane in two-way-bending (Sharma et al. 2018).

The combined effect of in-plane and OOP excitation may alter the performance of a wall. Little experimental research on this combined effect in URM may be found in literature, Najafgholipour et al. (2013) tested quasi-statically this combined effect on masonry wallettes while Dolatshahi and Aref (2016) on small URM piers. The absence of dynamic experimental investigations on this combined effect will drive the design of future tests of the herein described campaign.

Further shaking table tests on components are envisaged to be performed by EUCENTRE to study dynamic behaviour of secondary elements as chimneys and gables. Some research is already available in literature on similar topics, for example, the study presented by Giaretton et al. (2016).

### 4.2 Dynamic full-scale tests on structures

In the last three years, six full-scale unidirectional and bidirectional shake-table tests on different URM building typologies were conducted on: two cavity-wall terraced houses, one substructure, one roof (Graziotti et al. 2017; Tomassetti et al. 2018a; Correia et al. 2018; Miglietta et al. 2018) and two pre-1940s clay brick detached houses (Kallioras et al. 2018a, b). Another test on cavity-wall building is envisaged for the 2018 on EUCENTRE shaking table. By way of example, the following sections describe the test conducted in 2015 and 2016 on a cavity-wall terraced house (CAV-TH) and a clay brick detached house (CLAY-DH) representing two of the most diffuse typologies of the Groningen province. Rapid overviews of the specimens are given, focusing the attention more on the possible data obtainable from these types of test than specific analyses that could be found in dedicated works already published.

#### 4.2.1 Cavity-wall terraced house (CAV-TH)

This 56-t full-scale building specimen (Fig. 8a) was intended to represent the end unit of a 2-story unreinforced cavity-wall terraced house (CAV-TH) of the late 1970s, without specific seismic detailing. This building typology is characterized by wide openings along the front and back longitudinal walls, while blind loadbearing walls separate the units in the transverse direction. Figure 8b–d shows elevation views of the calcium silicate (CS) inner leaves. The inner load-bearing leaf of the cavity walls was made of CS bricks, while the outer leaf was a clay brick veneer; both leaves were built with 10-mm-thick mortar bed joints. An 8-cm gap was left between the two walls as in common practice. The pitched timber roof frame was supported by the transverse inner CS leaves (North and South sides) which extended above the second floor to form gables. Being the longitudinal walls more vulnerable to in-plane seismic excitation than transverse ones and being the gables out-of-plane response oriented in the same direction, the unidirectional shake-table test was performed in the longitudinal direction of the terraced house. The fundamental period of the undamaged structure resulted to be 0.17 s. Detailed description of the specimen can be found in Graziotti et al. (2017).

#### 4.2.2 Clay-brick detached house (CLAY-DH)

This 32-t full-scale building specimen (Fig. 9a) was designed to represent a pre-1940s URM detached house (CLAY-DH) of the Groningen province made of solid clay-brick walls and without any seismic detailing. The specimen was designed to include large asymmetrical openings in all the walls (Figs. 9, 10). The load-bearing structure consisted of 208-mm-thick URM walls built with the Dutch cross brickwork bond. A flexible timber diaphragm representing the typical flooring system of this typology in the building stock was adopted for the first floor. The roof external shape was designed to combine two different gables geometries: a full-height gable at the South façade and a jerkinhead roof with clipped gable at the North façade. These elements are more vulnerable when subjected to out-of-plane excitation because of weak connections to the roof framing along this direction: for this reason, the unidirectional shaking table test was performed perpendicularly to the gables, as shown by the arrows in Fig. 9. The fundamental period of the undamaged structure resulted to be 0.10 s. A detailed description of the specimen is reported in Kallioras et al. (2018b) while information regarding the data available upon request and their organization can be found in Kallioras et al. (2018c).

**Table 4** Specimen geometries for one-way, 1WB, and two-way-bending, 2WB, tested on shake table by EUCENTRE

| | Specimen ID | Wall type | w (m) | t (mm) | h (m) | $\sigma_v$ (MPa) | Input motion | No. ties/m$^2$ |
|---|---|---|---|---|---|---|---|---|
| 1WB | SIN-03-00 | Single CS leaf wall | 1.44 | 102 | 2.75 | 0.3 | Hor. | – |
| | SIN-01-00 | Single CS leaf wall | 1.44 | 102 | 2.75 | 0.1 | Hor. | – |
| | CAV-01-02 | CS inner wall | 1.44 | 102 | 2.75 | 0.1 | Hor. | 2 |
| | | Clay outer wall | 1.43 | 100 | 2.70 | 0 | | |
| | CAV-03-02 | CS inner wall | 1.44 | 102 | 2.75 | 0.3 | Hor. | 2 |
| | | Clay outer wall | 1.43 | 100 | 2.70 | 0 | | |
| | CAV-01-04 | CS inner wall | 1438 | 102 | 2.75 | 0.1 | Hor. | 4 |
| | | Clay outer wall | 1.43 | 100 | 2.70 | 0 | | |
| 2WB | CS-010/005-RR | Single CS leaf wall | 3.99 | 102 | 2.75 | 0.1/0.05 | Hor. | – |
| | CS-000-RF | Single CS leaf wall | 3.99 | 102 | 2.75 | 0 | Hor. | – |
| | CSW-000-RF | Single CS leaf wall | 3.99 | 102 | 2.75 | 0 | Hor. | – |
| | CL-000-RF | Single Clay leaf wall | 4.02 | 98 | 2.76 | 0 | Hor. | – |
| | CAV-000-RF | CS inner wall | 3.99 | 102 | 2.75 | 0 | Hor. | 2 |
| | | Clay outer wall | 4.39 | 98 | 2.76 | 0 | | |
| | CS-000-RFV | Single CS leaf wall | 3.99 | 102 | 2.75 | 0 | Hor. + Vert. | – |
| | CS-000-L1&L2 | Single CS leaf wall—L1 | 1.76 | 102 | 2.75 | 0 | Hor. | – |
| | | Single CS leaf wall—L2 | 2.21 | 102 | 2.75 | 0 | Hor. | – |
| | CS-000-RF2 | Single CS leaf wall | 3.99 | 102 | 2.75 | 0 | Hor. | – |

### 4.2.3 Mechanical properties of materials and components

A mechanical characterisation campaign is essential to feed the numerical models to be calibrated or verified (see Sect. 3.1). The mechanical characteristics of the two masonry typologies resulted to be in line with those observed in situ, in the Groningen province (see Sect. 2).

### 4.2.4 Instrumentation and testing protocol

Several instruments were installed on the specimens to monitor their structural response. The instrumentation of the CAV-TH specimen consisted of 33 accelerometers, 10 wire potentiometers, and 20 linear variable displacement transducers. The CLAY-DH was instead equipped with 37 accelerometers, 21 wire potentiometers, 37 displacement transducers, and a 3-dimensional optical acquisition system. A rigid steel frame was installed inside all the buildings. It did not interfere with the structures allowing their deformations during the dynamic tests. It served as a safety system, providing support in case of partial

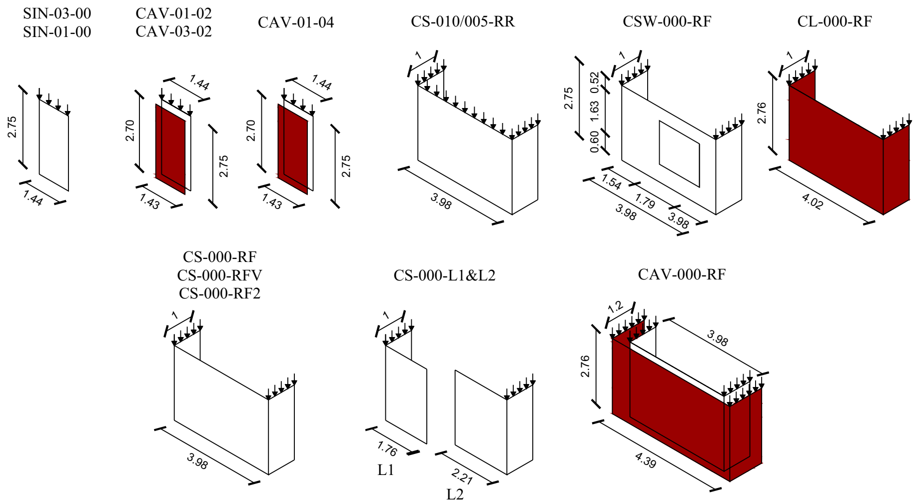


**Fig. 6** Summary scheme of specimens tested out-of-plane on shake table by EUCENTRE

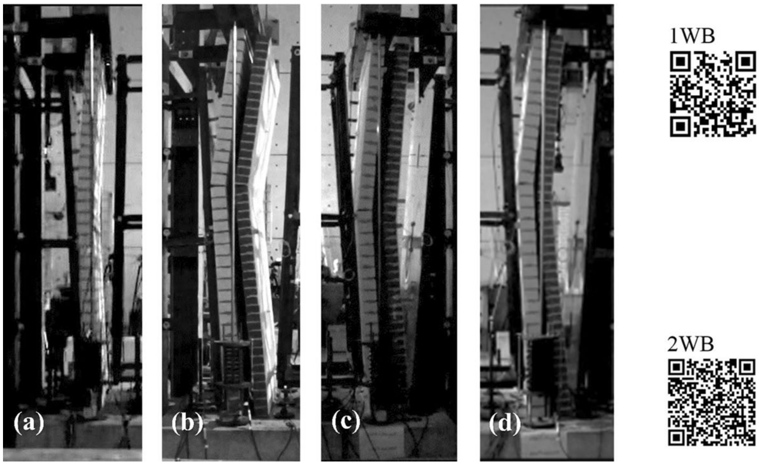


**Fig. 7** Snapshots of collapses in the OOP one-way-bending of specimens subjected to OOP shaking table tests (Graziotti et al. 2016a, b) and QR codes to visualize videos of OOP one-way- and two-way-bending shake table tests (EUCENTRE 2017)

or global collapse of the specimen, and constituted a rigid reference system for direct measurement of displacements relative to the shake-table.

Incremental dynamic tests with input motions of increasing intensity were performed to assess the behaviour of the building in terms of damage evolution, failure modes, and ultimate capacity. Two different input accelerograms were used, both characterised by smooth response spectra and short significant durations (defined as the time interval over which 5–75% of the total Arias intensity is developed, $D_{5-75}$). The first accelerogram labelled as SC1 was associated with a peak ground acceleration (PGA) of 0.096 g and $D_{5-75}=0.39$ s while the second accelerogram labelled as SC2 had a PGA of 0.155 g and $D_{5-75}=1.73$ s.

More details about the source of these two employed ground motions can be found in Bommer et al. (2015). Theoretical acceleration time-histories and the elastic pseudo-acceleration response spectra (5% damping) associated with both records can be seen in Fig. 11. Twelve significant input ground motions were obtained by scaling the acceleration amplitude of these accelerograms which constituted the testing sequence utilised for specimen CLAY-DH (Table 5).

#### 4.2.5 Damage evolution and damage states comparison

At the end of every shaking test, structural damage was surveyed in detail. Figures 12 and 13 shows the damage pattern after the last performed run for each of the two specimens. The cracks marked in black were pre-existing. A complete description of the damage evolution could be found in Graziotti et al. (2017) for CAV-TH and in Kallioras et al. (2018b) for CLAY-DH.

Table 6 summarizes the damage evolution of the two specimens: it reports the correspondence between global damage states defined by Grünthal (1998) and reached global drift ratio, *GDR*, defined as the second-floor displacement (relative to the base) divided by the second-floor height above the foundation for the CAV-TH building, or as the average first-floor displacement divided by the first-floor height for the CLAY-DH prototype. The damage thresholds are identified in relation to the maximum sustained input in terms of PGV and PGA for the two specimens.

#### 4.2.6 Hysteretic responses and dynamic behaviours

The hysteretic responses observed during the final test, represented in terms of base shear coefficient (defined as the base shear divided by the total weight of the specimen, *BSC*) and global drift ratio (*GDR*), are plotted in Fig. 14a. The weighted sum of the observed accelerations from each instrument was used to compute the *BSC*. In each case, the backbone response obtained are shown also.

Examining the response of the CAV-TH building, the first major sign of non-linear response was exhibited during the EQ2–150% test and was identified to be as a result of diffuse flexural cracks in the inner CS walls. Furthermore, significant nonlinear behaviour was shown during the EQ2–200% test as a result of widespread damage to the specimen. The ultimate *GDR*, defined as the maximum drift reached by the specimen before

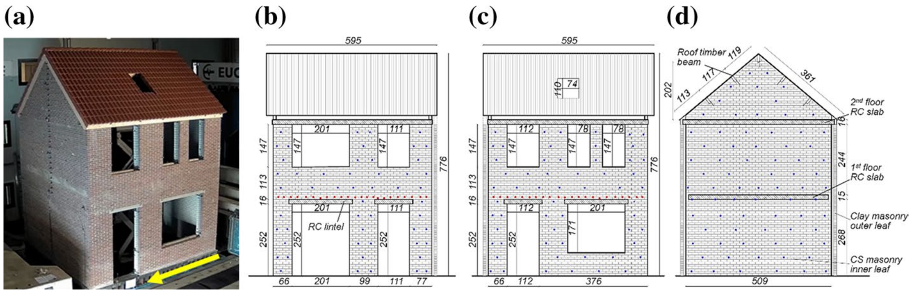


**Fig. 8** CAV-TH specimen: **a** Elevation views of the inner CS leaves of the CAV-TH specimen, **b** East side, **c** West side, **d** North and South sides. Blue dots represent ties between the two leaves (absent on the South side) (Graziotti et al. 2017)

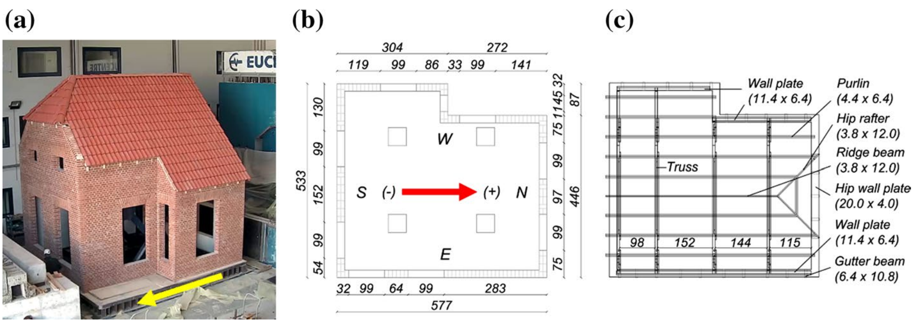


**Fig. 9** CLAY-DH specimen: **a** N–W view of the full-scale building; **b** first-floor plan; **c** roof framing. Coloured arrows indicate the positive direction of shaking (Kallioras et al. 2018b)

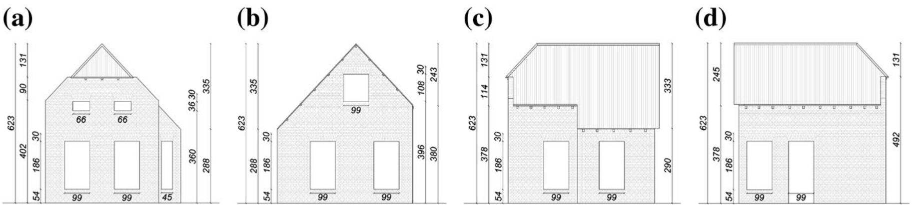


**Fig. 10** Elevation views of the CLAY-DH specimen: **a** North side, **b** South side, **c** West side, **d** East side (Kallioras et al. 2018b)

the decision to stop the test due to a near collapse condition, was found to be 0.70%. For the CLAY-DH specimen, non-linear response was initially observed during the SC2–250% test and became significantly exaggerated during the subsequent tests. This was identified to be as a result of a flexural-rocking mechanism that developed in West piers in addition to an out-of-plane behaviour of the gables. Kallioras et al. (2018b) reported the maximum recorded average first-floor drift ratio to be 0.94%.

Similar *GDRs* were observed in the two specimens when approaching near-collapse conditions. The CLAY-DH specimen, however, exhibited a higher lateral strength compared with the CAV-TH, with *BSCs* observed to be around 0.53 and 0.25, respectively. The incremental dynamic test (*IDT*) plot of Fig. 14b reflects this observation, where the CLAY-DH building resisted more than twice the PGA of the CAV-TH specimen at the near-collapse limit state.

## 5 Conclusions

This paper described the supporting methodology adopted to assess the seismic vulnerability of unreinforced masonry (URM) buildings in the Groningen province in the Netherlands by means of a comprehensive testing programme. In situ tests on different masonry typologies common in the building stock of the region, performed by EUCENTRE, TU Delft and TU Eindhoven with the collaboration of Arup, provided useful information to characterize the mechanical properties and their variability, which was useful in developing the exposure model and designing the laboratory tests. Systematic repetition of tests allowed the definition and proposal of a new procedure for the execution and interpretation of the in situ shear test for brick masonry: the so-called "shove test".

Quasi-static cyclic tests on structural members and assemblies, performed by EUCENTRE and TU Delft, represented an essential source of information allowing accurate investigation of several aspects related to their seismic response. They also constituted a valuable basis for the development of specific capacity models, strength criteria and limit state thresholds. Out-of-plane static and dynamic tests were also performed on cavity wall systems in one-way and two-way bending conditions. These pioneering tests represented an important benchmark with which to analyse the response of local mechanisms in existing URM buildings.

Six full-scale shaking table tests on structures (additional ones are scheduled for 2018 and 2019) were performed at the EUCENTRE and LNEC laboratories on entire building specimens or representative portions. Such tests, never before performed on similar structures subjected to induced seismicity records, were fundamental for assessing the modelling capabilities on complete building systems and directly allowed the study of their complex dynamic behaviour, specific energy dissipation characteristics, especially in the highly nonlinear range, and peculiar collapse modes. Some of these tests were conducted up to the collapse of the specimen in order to facilitate the calibration of both fragility and consequence models. The shaking table tests on building specimens also allowed for a direct comparison of the seismic vulnerability of specimens representing two of the most common building typologies. The solid-wall detached houses showed a lower seismic vulnerability due to a higher maximum base shear coefficient value of approximately 0.6 (compared to a value slightly less than 0.25 for the cavity-walls terraced houses). The near-collapse conditions were attained for values of peak ground acceleration ranging from 0.6 to 0.7 g for detached houses and from 0.3 to 0.4 g for terraced houses.

The experimental information collected during the tests constituted a basis for the development of numerical models and analytical tools used for predicting the behaviour of buildings belonging to the most common building typologies in the region (i.e. URM terraced buildings, typically with cavity walls and different diaphragm solutions depending on the construction period, and pre-1940 detached houses, with solid brick walls and timber diaphragms). These analyses were then used to derive the fragility curves used in the risk analysis process. All the reports, the majority of the videos and the data recorded by EUCENTRE and LNEC during the tests are available for interested researchers and stakeholders (they can be requested online at www.eucentre.it/nam-project).

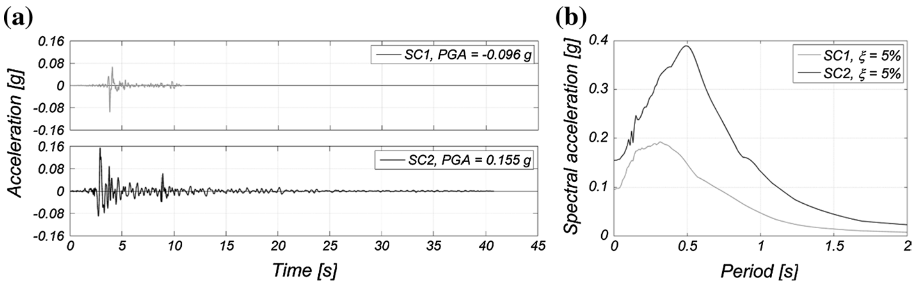


**Fig. 11** Input ground motions: **a** acceleration time histories, **b** elastic acceleration response spectra

**Table 5** Summary of the testing sequence

| Test input | Scale factor (%) | Nominal PGA (g) | Recorded PGA (g) | | Calculated PGV (mm/s) | |
|---|---|---|---|---|---|---|
| | | | CAV-TH | CLAY-DH | CAV-TH | CLAY-DH |
| SC1 | 25 | 0.024 | 0.024 | 0.026 | 15 | 22 |
| SC1 | 50 | 0.05 | 0.05 | 0.05 | 31 | 35 |
| SC1 | 100 | 0.01 | 0.01 | 0.10 | 56 | 58 |
| SC1 | 150 | 0.14 | 0.14 | 0.15 | 77 | 86 |
| SC2 | 50 | 0.08 | 0.09 | 0.08 | 67 | 73 |
| SC2 | 100 | 0.16 | 0.17 | 0.14 | 123 | 122 |
| SC2 | 125[a] | 0.20 | 0.19 | – | 133 | – |
| SC2 | 150 | 0.24 | 0.24 | 0.23 | 164 | 186 |
| SC2 | 200 | 0.32 | 0.31 | 0.29 | 218 | 241 |
| SC2 | 250[b] | 0.40 | – | 0.39 | – | 308 |
| SC2 | 300[b] | 0.48 | – | 0.50 | – | 365 |
| SC2 | 400[b] | 0.64 | – | 0.68 | – | 467 |

*PGA* peak ground acceleration, *PGV* peak ground velocity

[a]Only for the CAV-TH specimen

[b]Only for the CLAY-DH specimen

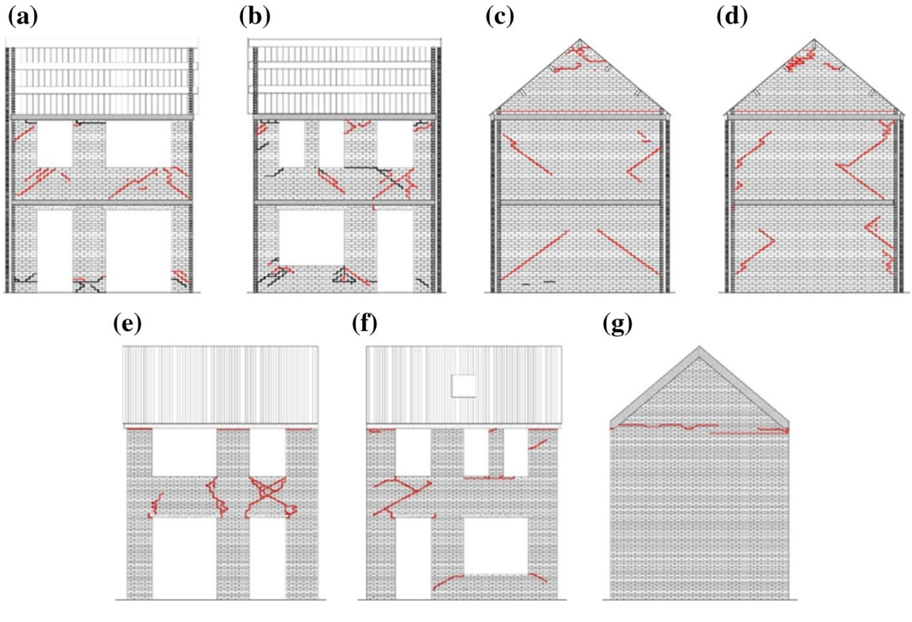


**Fig. 12** Crack pattern on the CAV-TH specimen after the SC2-200% test (PGA = 0.31 g): **a** East CS wall, **b** West CS wall, **c** North CS wall, **d** South CS wall, **e** East clay façade, **f** West clay façade, **g** North clay façade (Graziotti et al. 2017)

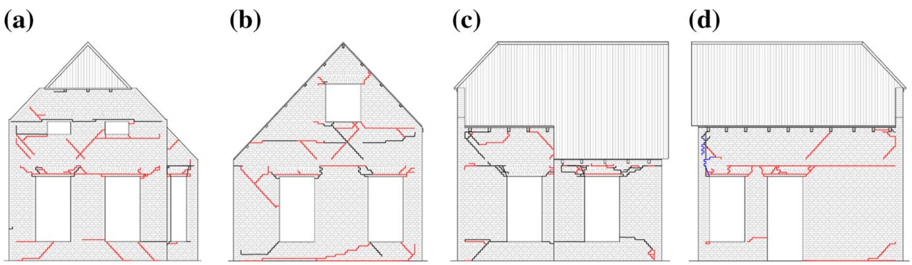


**Fig. 13** Crack pattern on the CLAY-DH specimen after the SC2-400% test (PGA = 0.68 g): **a** North wall, **b** South wall, **c** West wall, **d** East wall (Kallioras et al. 2018b)

**Table 6** Correspondence between damage states, reached global drift ratio and maximum sustained input in terms of PGV and PGA for the two specimens

| | Global drift ratio (%) | | PGV (mm/s) | | PGA (g) | |
|---|---|---|---|---|---|---|
| | CAV-TH | CLAY-DH | CAV-TH | CLAY-DH | CAV-TH | CLAY-DH |
| Global structural damage | | | | | | |
| None | 0.05 | 0.01 | 77 | 110 | 0.14 | 0.14 |
| Minor | 0.07 | 0.04 | 123 | 297 | 0.17 | 0.39 |
| Moderate | 0.23 | 0.25 | 164 | 346 | 0.24 | 0.50 |
| Extensive | 0.73 | 0.94 | 218 | 444 | 0.31 | 0.68 |

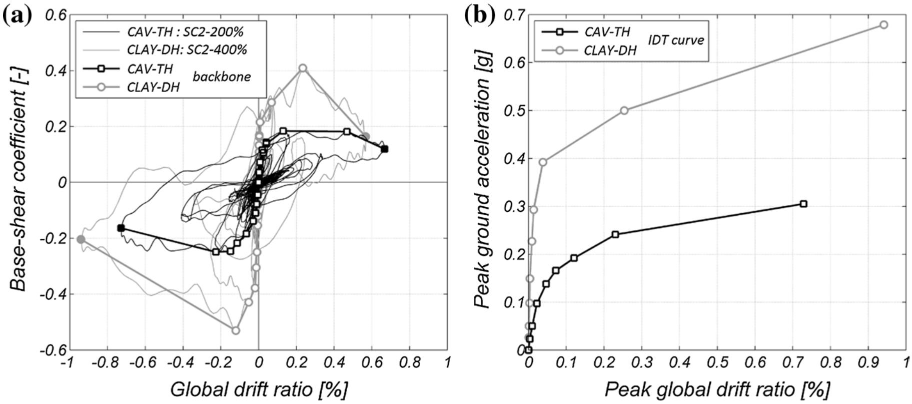


**Fig. 14** Response of the two specimens: **a** hysteretic behaviour, **b** IDT curves (Guerrini et al. 2017)

**Acknowledgements** This work is part of the EUCENTRE project "Study of the vulnerability of masonry buildings in Groningen", within the research programme framework on hazard and risk of induced seismicity in the Groningen province, sponsored by the Nederlandse Aardolie Maatschappij BV (NAM). The authors would like to thank all parties involved in this project: the DICAr Laboratory of the University of Pavia and the EUCENTRE Laboratory, which performed the tests; and partners NAM, Arup, TU Delft and TU Eindhoven for their insight and contributions related to the test programme. The valuable advice of R. Pinho was essential to the project and is gratefully acknowledged. Thanks also go to J. Uilenreef, A.

Campos Costa, P.X. Candeias, A.A. Correia, H. Crowley, F. Dacarro, A. Fragomeli, S. Girello, G. Guerrini, L. Grottoli, S. Kallioras, M. Mandirola, B. Marchesi, M. Miglietta, G. O'Reilly, S. Peloso, A. Rossi, S. Sharma, G. Sinopoli and U. Tomassetti for the practical support. Discussions with Prof. M.C. Griffith have been a valuable reference in several stages of the project. The authors would also like to thank two anonymous reviewers for their comments, which certainly contributed to an improvement of the manuscript.

## References

Andreotti G, Graziotti F, Magenes G (2018) Detailed micro-modelling of the direct shear tests of brick masonry specimens: the role of dilatancy. Eng Struct 168:929–949

ASTM C1196-14a (2014a) Standard test method for in situ compressive stress within solid unit masonry estimated using Flatjack measurements. ASTM International, West 612 Conshohocken, PA. www.astm.org. https://doi.org/10.1520/c1196-14a

ASTM C1197-14a (2014b) Standard test method for in-situ measurement of masonry deformability properties using the Flatjack method. ASTM International, West 612 Conshohocken, PA. www.astm.org. https://doi.org/10.1520/c1197-14a

ASTM C1531-16 (2016). Standard test methods for in-situ measurement of masonry mortar joint shear strength index. ASTM International, West Conshohocken, PA. www.astm.org. https://doi.org/10.1520/c1531-16

Avanes C, Fusco C, Asghari Mooneghi M, Huang Y, Palmieri M, Sturt R (2018) LS-DYNA numerical simulation of full scale masonry cavity wall terraced house tested dynamically. In: Proceedings of the 16th European conference on earthquake engineering, 16ECEE, 18-21/6, Thessaloniki, Greece

Bommer JJ, Crowley H (2017) The purpose and definition of the minimum magnitude limit in PSHA calculations. Seismol Res Lett 88(4):1097–1106

Bommer JJ, Crowley H, Pinho R, Polidoro B (2015) Selection of acceleration time-series for shake table testing of Groningen masonry building at the EUCENTRE, Pavia. Report—Groningen Field Seismic Hazard and Risk Assessment Project, EUCENTRE, Pavia, Italy

Bommer JJ, Dost B, Edwards B, Stafford PJ, van Elk J, Doornhof D, Ntinalexis M (2016) Developing an application-specific ground motion model for induced seismicity. Bull Seismol Soc Am 106(1):158–173

Bonura V, Jafari S, Zapico Blanco B, Graziotti F (2018) Interpretation of in situ shear test for brick masonry: a benchmark study. In: Proceedings of the 16th European conference on earthquake engineering, 16ECEE, 18-21/6, Thessaloniki, Greece

Bourne SJ, Oates SJ, Bommer JJ, Dost B, van Elk J, Doornhof D (2015) A Monte Carlo method for probabilistic hazard assessment of induced seismicity due to conventional natural gas production. Bull Seismol Soc Am 105(3):1721–1738

Brunesi E, Peloso S, Pinho R, Nascimbene R (2018a) Cyclic testing of a full-scale two-storey reinforced precast concrete wall–slab–wall structure. Bull Earthq Eng. https://doi.org/10.1007/s10518-018-0359-z

Brunesi E, Peloso S, Pinho R, Nascimbene R (2018b) Cyclic testing and analysis of a full-scale cast-in-place reinforced concrete wall-slab-wall structure. Bull Earthq Eng. https://doi.org/10.1007/s10518-018-0374-0

Brunesi E, Peloso S, Pinho R, Nascimbene R (2018c) Dynamic shake-table testing of a full-scale two-storey reinforced precast concrete wall–slab–wall structure. Earthq Spectra (In review)

Calvi GM, Kingsley GR, Magenes G (1996) Testing of masonry structures for seismic assessment. Earthq Spectra 12(1):145–162

Correia AA, Tomassetti U, Penna A, Magenes G, Graziotti F (2018) Collapse shake-table test on a URM-timber roof substructure. In: Proceedings of the 16th European conference on earthquake engineering, 16ECEE, 18-21/6, Thessaloniki, Greece

Crowley H, Pinho R (2017) Report on the v5 fragility and consequence models for the Groningen field. Report—Groningen Field Seismic Hazard and Risk Assessment Project. www.nam.nl/feiten-en-cijfers/onderzoeksrapporten.html

Crowley H, Pinho R, Polidoro B, van Elk J (2017a) Developing fragility and consequence models for buildings in the Groningen field. Neth J Geosci 96(5):s247–s257

Crowley H, Polidoro B, Pinho R, van Elk J (2017b) Framework for developing fragility and consequence models for local personal risk. Earthq Spectra 33(4):1325–1345

Crowley H, Pinho R, van Elk J, Uilenreef J (2018) Probabilistic damage assessment of buildings due to induced seismicity. Bull Earthq Eng. https://doi.org/10.1007/s10518-018-0462-1
Degli Abbati S, Lagomarsino S (2017) Out-of-plane static and dynamic response of masonry panels. Eng Struct 150:803–820
Dolatshahi KM, Aref AJ (2016) Multi-directional response of unreinforced masonry walls: experimental and computational investigations. Earthq Eng Struct Dyn 45(9):1427–1449
Dost B, Edwards B, Bommer JJ (2018) The relationship between M and ML: a review and application to induced seismicity in the Groningen gas field, The Netherlands. Seismol Res Lett 89(3):1062–1074
EN 1015-11 (1999) Methods of test for mortar for masonry—Part 11: determination of flexural and compressive strength of hardened mortar. European Standards, CEN/TC, Brussels
EN 1052-1 (1998) Methods of test for masonry—Part 1: determination of compressive strength. European Standards, CEN/TC, Brussels
EN 1052-2 (1999) Methods of test for masonry—Part 2: determination of flexural strength. European Standards, CEN/TC, Brussels
EN 1052-3 (2002) Methods of test for masonry—Part 3: determination of initial shear strength. European Standards, CEN/TC, Brussels
EN 1052-5 (2005) Methods of test for masonry—Part 5: determination of bond strength by the bond wrench method. European Standards, CEN/TC, Brussels
EN 772-1 (2011) Methods of test for masonry units—Part 1: determination of compressive strength. European Standards, CEN/TC, Brussels
Esposito R, Terwel KC, Ravenshorst GJP, Schipper HR, Messali F, Rots JG (2017) Cyclic pushover test on an unreinforced masonry structure resembling a typical Dutch terraced house. In: Proceedings of 16th World conference on earthquake engineering, 16WCEE, Santiago, CL
Esposito R, Messali F, Ravenshorst GJP, Schipper HR, Rots JG (2018) Can wind-resistant URM buildings withstand shallow earthquakes? The case study of a Dutch terraced house. Bull Earthq Eng (In Review)
EUCENTRE (2017) URM walls in out-of-plane two-way bending. YouTube video playlist. https://www.youtube.com/watch?v=Qg5WUyRX2IA&list=PLRDMVFxhFvQnMRn7SDXreqbcg044logeB&index=4
Giaretton M, Dizhur D, Ingham JM (2016) Shaking table testing of as-built and retrofitted clay brick URM cavity-walls. Eng Struct 125:70–79
Gillian R, Miles P, Bruce R, Richard J (2018) Global review of human-induced earthquakes. Earth Sci Rev 178:438–514
Graziotti F, Rossi A, Mandirola M, Penna A, Magenes G (2016a) Experimental characterization of calcium-silicate brick masonry for seismic assessment. In: Proceedings of the 16th international brick and block masonry conference (IBMAC), Padova, Italy
Graziotti F, Tomassetti U, Penna A, Magenes G (2016b) Out-of-plane shaking table tests on URM single leaf and cavity walls. Eng Struct 125:455–470
Graziotti F, Tomassetti U, Kallioras S, Penna A, Magenes G (2017) Shaking table test on a full scale URM cavity wall building. Bull Earthq Eng 15(12):5329–5364
Graziotti F, Tomassetti U, Sharma S, Grottoli L, Magenes G (2018a) Experimental response of URM single leaf and cavity walls in out-of-plane two-way bending generated by seismic excitation. Constr Build Mater (accepted)
Graziotti F, Guerrini G, Rossi A, Andreotti G, Magenes G (2018b) Proposal for an improved procedure and interpretation of ASTM C1531 for the in situ determination of brick-masonry shear strength. ASTM Selected Technical Papers: 2018 Masonry Symposium, San Diego, CA, USA
Griffith MC, Vaculik J, Lam NTK, Wilson J, Lumantarna E (2007) Cyclic testing of unreinforced masonry walls in two-way bending. Earthq Eng Struct Dyn 36(6):801–821
Grünthal G (1998) Editor. European Macroseismic Scale 1998—EMS-98. Cahiers du Centre Européen de Géodynamique et de Séismologie 15. Centre Européen de Géodynamique et de Séismologie, LUX
Guerrini G, Graziotti F, Penna A, Magenes G (2017) Dynamic shake-table tests on two full-scale, unreinforced masonry buildings subjected to induced seismicity. In: International conference on experimental vibration analysis for civil engineering structures. Springer, Cham, pp 376–387
Hancock J, Bommer JJ (2006) A state-of-knowledge review of the influence of strong-motion duration on structural damage. Earthq Spectra 22(3):827–845
Housner GW (1952) Intensity of ground motion during strong earthquakes. Technical Report, California Institute of Technology, California, USA. http://authors.library.caltech.edu
Jafari S, Rots JG, Esposito R, Messali F (2017) Characterizing the material properties of Dutch unreinforced masonry. Procedia Eng 193:250–257

Kallioras S (2017) Numerical simulation of shaking table tests on a URM cavity-wall building. Mason Int 30(2):39–48

Kallioras S, Correia AA, Marques AI, Candeias P, Graziotti F (2018a) LNEC-BUILD-3: experimental investigation of the seismic response of a Dutch URM detached house with chimneys. Technical Report, EUCENTRE, Pavia, Italy

Kallioras S, Guerrini G, Tomassetti U, Marchesi B, Penna A, Graziotti F, Magenes G (2018b) Experimental seismic performance of a full-scale unreinforced clay-masonry building with flexible timber diaphragms. Eng Struct 161:231–249

Kallioras S, Guerrini G, Tomassetti U, Peloso S, Graziotti F (2018c) Dataset from the dynamic shake-table test of a full-scale unreinforced clay–masonry building with flexible timber diaphragms. Data Brief 18:629–640

Lagomarsino S, Penna A, Galasco A, Cattari S (2013) TREMURI program: an equivalent frame model for the nonlinear seismic analysis of masonry buildings. Eng Struct 56:1787–1799

Malomo D, Comini P, Pinho R, Penna A (2018a) The applied element method and the modelling of both in-plane and out-of-plane response of URM walls. In: Proceedings of the 16th European Conference on Earthquake Engineering, 16ECEE, 18-21/6, Thessaloniki, Greece

Malomo D, Pinho R, Penna A (2018b) Using the applied element method for modelling calcium silicate brick masonry subjected to in-plane cyclic loading. Earthq Eng Struct Dyn 47(7):1610–1630

Malomo D, Pinho R, Penna A (2018c) Using the applied element method to simulate the dynamic response of full-scale URM houses tested to collapse or near-collapse conditions. In: Proceedings of the 16th European Conference on Earthquake Engineering, 16ECEE, 18-21/6, Thessaloniki, Greece

Mandirola M, Kallioras S, Tomassetti U, Graziotti F (2017) Tests on URM clay and calcium silicate masonry structures: identification of damage limit states, Technical Report (Working version of October 2017), EUCENTRE, Pavia, Italy

Messali F, Ravenshorst G, Esposito R, Rots J (2017) Large-scale testing program for the seismic characterization of Dutch masonry walls. In: Proceedings of the 16th European Conference on Earthquake Engineering, 16WCEE, Santiago, CL

Messali F, Esposito R, Jafari S, Ravenshorst GJP, Korswagen P, Rots J (2018). A multiscale experimental characterisation of Dutch unreinforced masonry buildings. In: Proceedings of 16th European Conference on Earthquake Engineering (ECEE), 18–21 June, Thessaloniki, Greece

Miglietta M, Graziotti F, Guerrini G, Tomassetti U, Grottoli L, Mazzella L, Magenes G. (2018) Shake-table test on a cavity-wall building with flexible diaphragms. Report, EUCENTRE, Pavia, Italy

Najafgholipour MA, Maheri MR, Lourenço PB (2013) Capacity interaction in brick masonry under simultaneous in-plane and out-of-plane loads. Constr Build Mater 38:619–626

NAM (2016) Technical Addendum to the Winningsplan 2016. http://www.nam.nl/feiten-en-cijfers/onderzoeksrapporten.html

Rossi A, Graziotti F, Magenes G (2015) A proposal for the interpretation of the in-situ shear strength index test for brick masonry. In: Proceedings of the XVI ANIDIS Conference, L'Aquila, Italy

Sharma S, Grottoli L, Tomassetti U, Graziotti F (2018) Out-of-plane two-way bending shaking table tests on single leaf and cavity walls. Technical Report, EUCENTRE, Pavia, Italy. http://www.eucentre.it/project-nam/

Tomassetti U, Correia A, Candeias PX, Graziotti F, Campos Costa A (2018a) Two-way bending out-of-plane collapse of a full-scale URM building tested on a shake table. Bull Earthq Eng (in review)

Tomassetti U, Graziotti F, Penna A, Magenes G (2018b) Modelling one-way out-of-plane response of single-leaf and cavity walls. Eng Struct 167:241–255

Tondelli M, Graziotti F, Rossi A, Magenes G (2015) Characterization of masonry materials in the Groningen area by means of in situ and laboratory testing. Technical Report, EUCENTRE, Pavia, Italy. http://www.eucentre.it/nam-project

Vaculik J (2012) Unreinforced masonry walls subjected to out-of-plane seismic actions. PhD Thesis, Univ. of Adelaide, AU

Vaculik J, Griffith MC (2018) Out-of-plane shaketable testing of unreinforced masonry walls in two-way bending. Bull Earthq Eng 16:2839–2876

van Elk J, Doornho D, Bommer JJ, Bourne SJ, Oates SJ, Pinho R, Crowley H (2017) Hazard and risk assessments for induced seismicity in Groningen. Neth J Geosci 96(5):s259–s269

Zapico Blanco B, Tondelli M, Jafari S, Graziotti F, Millekamp H, Rots J, Palmieri M (2018) A Masonry Catalogue for the Groningen Region. In: Proceedings of the 16th European Conference on Earthquake Engineering, 16ECEE, 18-21/6, Thessaloniki, Greece